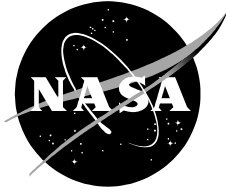NASA/TM-2004-213277

An Interface Damage Model for the Simulation of Delamination Under Variable-Mode Ratio in Composite Materials

Albert Turon
University of Girona, Girona, Spain

Pedro P. Camanho
University of Porto, Porto, Portugal

Josep Costa
University of Girona, Girona, Spain

Carlos G. Dávila
NASA Langley Research Center, Hampton, Virginia

October 2004

The NASA STI Program Office ... in Profile

Since its founding, NASA has been dedicated to the advancement of aeronautics and space science. The NASA Scientific and Technical Information (STI) Program Office plays a key part in helping NASA maintain this important role.

The NASA STI Program Office is operated by Langley Research Center, the lead center for NASA's scientific and technical information. The NASA STI Program Office provides access to the NASA STI Database, the largest collection of aeronautical and space science STI in the world. The Program Office is also NASA's institutional mechanism for disseminating the results of its research and development activities. These results are published by NASA in the NASA STI Report Series, which includes the following report types:

TECHNICAL PUBLICATION. Reports of completed research or a major significant phase of research that present the results of NASA programs and include extensive data or theoretical analysis. Includes compilations of significant scientific and technical data and information deemed to be of continuing reference value. NASA counterpart of peer-reviewed formal professional papers, but having less stringent limitations on manuscript length and extent of graphic presentations.

TECHNICAL MEMORANDUM. Scientific and technical findings that are preliminary or of specialized interest, e.g., quick release reports, working papers, and bibliographies that contain minimal annotation. Does not contain extensive analysis.

CONTRACTOR REPORT. Scientific and technical findings by NASA-sponsored contractors and grantees.

CONFERENCE PUBLICATION. Collected papers from scientific and technical conferences, symposia, seminars, or other meetings sponsored or co-sponsored by NASA.

SPECIAL PUBLICATION. Scientific, technical, or historical information from NASA programs, projects, and missions, often concerned with subjects having substantial public interest.

TECHNICAL TRANSLATION. English-language translations of foreign scientific and technical material pertinent to NASA's mission.

Specialized services that complement the STI Program Office's diverse offerings include creating custom thesauri, building customized databases, organizing and publishing research results ... even providing videos.

For more information about the NASA STI Program Office, see the following:
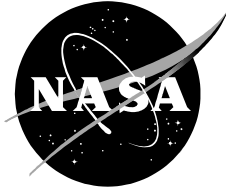
Access the NASA STI Program Home Page at *http://www.sti.nasa.gov*

E-mail your question via the Internet to help@sti.nasa.gov

Fax your question to the NASA STI Help Desk at (301) 621-0134

Telephone the NASA STI Help Desk at (301) 621-0390

Write to:
NASA STI Help Desk
NASA Center for AeroSpace Information
7121 Standard Drive
Hanover, MD 21076-1320

NASA/TM-2004-213277

An Interface Damage Model for the Simulation of Delamination Under Variable-Mode Ratio in Composite Materials

Albert Turon
University of Girona, Girona, Spain

Pedro P. Camanho
University of Porto, Porto, Portugal

Josep Costa
University of Girona, Girona, Spain

Carlos G. Dávila
NASA Langley Research Center, Hampton, Virginia

October 2004

Acknowledgments

Available from:

NASA Center for AeroSpace Information	National Technical Information Service
7121 Standard Drive	5285 Port Royal Road
Hanover, MD 21076-1320	Springfield, VA 22161
301-621-0390	703-605-6000

An Interface Damage Model for the Simulation of Delamination under Variable-Mode Ratio in Composite Materials

A. Turon [a] , P.P. Camanho [b] , J. Costa [a] , C.G. Dávila [c]

[a] *AMADE, Polytechnic School, University of Girona, Campus Montilivi s/n, 17071 Girona, Spain*

[b] *DEMEGI, Faculdade de Engenharia, Universidade do Porto, Rua Dr. Roberto Frias, 4200-465, Porto, Portugal*

[c] *NASA Langley Research Center, Hampton, Virginia, U.S.A.*

Abstract

A thermodynamically consistent damage model for the simulation of progressive delamination under variable mode ratio is presented. The model is formulated in the context of the Damage Mechanics. The constitutive equation that results from the definition of the free energy as a function of a damage variable is used to model the initiation and propagation of delamination. A new delamination initiation criterion is developed to assure that the formulation can account for changes in the loading mode in a thermodynamically consistent way. The formulation proposed accounts for crack closure effects avoiding interfacial penetration of two adjacent layers after complete decohesion. The model is implemented in a finite element formulation. The numerical predictions given by the model are compared with experimental results.

1   Introduction

Delamination is one of the most common types of damage in laminated fibre-reinforced composites due to their relatively weak interlaminar strengths. Delamination may arise under various circumstances, such as in the case of transverse concentrated loads caused by low velocity impacts.

Structural collapse in a composite structure is often caused by the evolution of different types of damages created in a local zone of the structure. The particular damage modes depend upon loading, lay-up and stacking sequence. Delamination is often a significant contributor to the collapse of a structure

[1]. Moore et al. [2] justify the need to account for delamination from the point of view of Fracture Mechanics: the energy release rates necessary for failure of a composite part from intralaminar and interlaminar damage were computed and the results showed that the lowest energy release rate obtained was for delamination.

When other material non-linearities can be neglected, methods based on Linear Elastic Fracture Mechanics (LEFM) have been proven to be effective in predicting delamination growth. However, LEFM cannot be applied without an initial crack. In many situations, stress-based methods have been applied to predict the initiation of delaminations, and after the delamination onset, Fracture Mechanics can be used to describe delamination growth [3]-[4]. Techniques such as virtual crack closure technique (VCCT) [5]-[9], J-integral method [10], virtual crack extension [11] and stiffness derivative [12] have often been used. These techniques have in common that the delamination is assumed to propagate when the associated energy release rate is greater than or equal to a critical value [13]. However, difficulties are also encountered when these techniques are implemented using finite element codes. The calculation of fracture parameters, e.g. stress intensity factors or energy release rates, requires nodal variable and topological information from the nodes ahead and behind the crack front. Such calculations can be done with some effort for a stationary crack, but can be extremely difficult when progressive crack propagation is involved.

Another approach to the numerical simulation of the delamination can be developed within the framework of Damage Mechanics. Models formulated using Damage Mechanics are based on the concept of the cohesive crack model: a cohesive damage zone or softening plasticity is developed near the crack front. The origin of the cohesive crack model goes back to Dugdale [14] who introduced the concept that stresses in the material are limited by the yield stress and that a thin plastic is generated in front of the notch. Barenblatt [15] introduced cohesive forces on a molecular scale in order to solve the problem of equilibrium in elastic bodies with cracks. Hillerborg et al. [16] proposed a model similar to the Barenblatt model, but where the concept of tensile strength was introduced. Hillerborg's model allowed for existing cracks to grow and, even more importantly, also allowed for the initiation of new cracks.

Cohesive damage zone models relate tractions to displacement jump at an interface where a crack may occur. Damage initiation is related to the interfacial strength, i.e., the maximum traction on the traction-displacement jump curve. When the area under the traction/displacement jump curve is equal to the fracture toughness, the traction is reduced to zero and new crack surface formed. The advantages of cohesive zone models are their simplicity and the unification of crack initiation and growth within one model. Moreover, cohesive zone formulations can also be easily implemented in finite element codes

using decohesion elements [17]-[25].

In the formulation of the cohesive models, it is important to control the energy dissipation during delamination growth in order to avoid the restoration of the cohesive state, i.e., it is necessary to assure that the model satisfies the Clausius-Duhem inequality. There are some models in the literature that can be used under mixed-mode conditions [21],[23]-[24], [29]-[34], but some of them do not satisfy the Clausius-Duhem inequality under variable-mode loading situation.

A damage model for the simulation of delamination under variable-mode is presented in this paper. A new delamination initiation criterion is developed from the expression of the critical energy release rate for delamination propagation under mixed-mode loading presented in [35]. The model is implemented into the commercial finite element code ABAQUS by means of a user-written decohesion element.

This paper is structured as follows: first, the formulation of the delamination onset and growth model is presented. Afterward, the delamination damage model is formulated and the initiation and propagation surfaces are defined. The finite element discretization of the boundary value problem is based on the variational formulation of the local form of momentum balance. Finally, the numerical predictions are compared with experimental results.

2   Model for delamination onset and propagation

The boundary value problem, the kinematic equations, and the constitutive relations are presented for the formulation of the model for delamination onset and delamination propagation.

2.1   Boundary value problem

Consider a domain Ω, as shown in figure 1(a), containing a crack Γ_c. The part of the crack on which a cohesive law is active is denoted by Γ_{coh} and is called the fracture process zone (FPZ).

Prescribed tractions, F_i, are imposed on the boundary Γ_F, whereas prescribed displacements are imposed on Γ_u. The stress field inside the domain, σ_{ij}, is related to the external loading and the closing tractions τ_j^+, τ_j^- in the cohesive zone through the equilibrium equations:

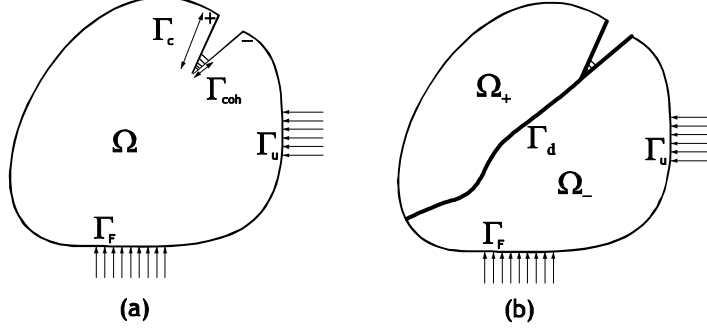$$\sigma_{ij,j} = 0 \text{ on } \Omega \tag{1}$$

3

Fig. 1. *Body Ω crossed by a material discontinuity Γ_d in the undeformed configuration*

$$\sigma_{ij} n_j = t_i \text{ on } \Gamma_F \tag{2}$$

$$\sigma_{ij} n_j^+ = \tau_i^+ = -\tau_i^- = \sigma_{ij} n_j^- \text{ on } \Gamma_{coh} \tag{3}$$

2.2 *Kinematics of the interfacial surface*

To develop the necessary kinematic relationships, consider the crack Γ_c shown in Figure 1(a) part of a material discontinuity, Γ_d, which divides the domain Ω into two parts, Ω_+ and Ω_- (Figure 1(b)).

The displacement jump $[\![u_i]\!]$ across the material discontinuity Γ_d can be written as:

$$[\![u_i]\!] = u_i^+ - u_i^- \tag{4}$$

where $u_i^\pm$ denotes the displacement of the points on the surface of the material discontinuity Γ_d of the part $\Omega_\pm$ of the domain.

The fundamental problem introduced by the interfacial surface Γ_d is how to express the virtual displacement jumps associated to the surfaces $\Gamma_{d\pm}$ as a function of the virtual displacements. Consider a three-dimensional space with Cartesian coordinates X_i, $i = 1, 2, 3$. Let the Cartesian coordinates $x_i^\pm$ describe the deformation of the upper and lower surfaces $\Gamma_{d\pm}$ in the deformed configuration. Any material point on $\Gamma_{d\pm}$ in the deformed configuration is related to its undeformed configuration through:

$$x_i^\pm = X_i + u_i^\pm \tag{5}$$

where $u_i^\pm$ are displacements quantities with respect to the fixed Cartesian coordinate system. Then, the coordinates $\bar{x}_i$ of the midsurface can be written as:

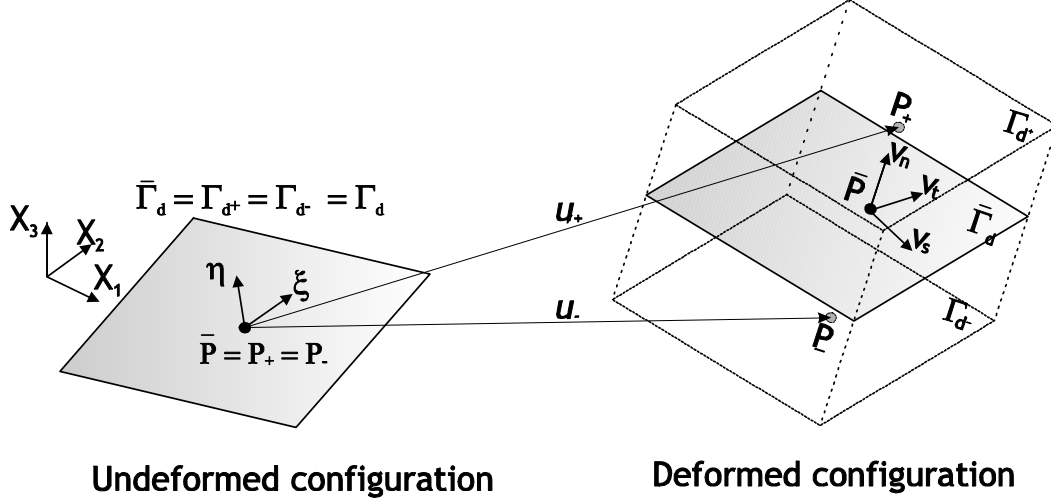$$\bar{x}_i = X_i + \frac{1}{2}\left(u_i^+ + u_i^-\right) \tag{6}$$

4

Fig. 2. *Interfacial surface deformation*

The components of the displacement jump vector are evaluated at the mid-surface $\bar{\Gamma}_d$, which is coincident with Γ_d in the undeformed configuration (see figure 2). The midsurface coordinate gradients define the components of the two vectors, v_{η_i} and v_{ξ_i}, that define the tangential plane at a given point, $\bar{P}$:

$$v_{\eta_i} = \bar{x}_{i,\eta} \tag{7}$$

$$v_{\xi_i} = \bar{x}_{i,\xi} \tag{8}$$

where η, ξ are curvilinear coordinates on the surface $\bar{\Gamma}_d$. Although v_{η_i} and v_{ξ_i} are generally not orthogonal to each other, their vector product defines a surface normal. Therefore, the local normal coordinate vector is obtained as:

$$\mathbf{v}_n = \mathbf{v}_\xi \times \mathbf{v}_\eta \left\| \mathbf{v}_\xi \times \mathbf{v}_\eta \right\|^{-1} \tag{9}$$

The tangential coordinates are then obtained as:

$$\mathbf{v}_s = \mathbf{v}_\xi \left\| \mathbf{v}_\xi \right\|^{-1} \tag{10}$$

$$\mathbf{v}_t = \mathbf{v}_n \times \mathbf{v}_s \tag{11}$$

The components of $\mathbf{v}_n$, $\mathbf{v}_s$ and $\mathbf{v}_t$ represent the direction cosines of the local coordinate system in the global coordinate system at a material point $\bar{P} \in \bar{\Gamma}_d$. The director cosines define the following rotation tensor Θ_{mi}, expressed in Voigt notation as:

$$\boldsymbol{\Theta} = \left[\mathbf{v}_n, \mathbf{v}_s, \mathbf{v}_t \right] \tag{12}$$

Θ is orthogonal and relates the local coordinate system to the fixed coordinate system. Using the rotation tensor, the normal and tangential components of the displacement jump tensor expressed in terms of the displacement field in

5

global coordinates are:

$$\Delta_m = \Theta_{mi} [\![u_i]\!] \tag{13}$$

Δ_m is the displacement jump tensor in the local coordinate system.

The deformed differential surface area of the midsurface $d\bar{\Gamma}_d$ is expressed in the form:

$$d\bar{\Gamma}_d = \| \mathbf{v}_\xi \times \mathbf{v}_\eta \| \, d\Gamma_d^0 = J d\Gamma_d^0 \tag{14}$$

where $d\Gamma_d^0$ is the differential undeformed surface area.

2.3   Constitutive laws

A constitutive law relating the cohesive tractions, τ_j, to the displacement jump in the local coordinates, Δ_i, is required for modelling the constitutive behaviour of the material discontinuity. The constitutive laws in the material discontinuity may be formally written:

$$\tau_j = \tau \left(\Delta_i \right) \tag{15}$$

$$\dot{\tau}_j = D_{ji}^{\mathrm{tan}} \dot{\Delta}_i \tag{16}$$

where D_{ji}^{tan} is the constitutive tangent stiffness tensor.

A new constitutive model relating the displacement jumps to the tractions, and based on Damage Mechanics is proposed.

The delamination model proposed follows the general formulation of Continuum Damage Models proposed by Simo and Ju [36]-[37] and Mazars [38].

The free energy per unit volume of the interface is defined as:

$$\psi \left(\Delta, \mathsf{d} \right) = \left(1 - \mathsf{d} \right) \psi^0 \left(\Delta \right) \tag{17}$$

where d is the damage variable and ψ^0 is a convex function in the displacement jump space defined as:

$$\psi^0 \left(\Delta \right) = \frac{1}{2} \Delta_i D_{ij}^0 \Delta_j \tag{18}$$

Negative values of Δ_3 do not have any physical meaning because interpenetration is prevented by contact. Therefore negative values of Δ_3 should not have any influence in the variation of the free energy of the interface. Thus, a modification of equation (17) is proposed to prevent interfacial penetration of the two adjacent layers after complete decohesion. The expression for the free energy per unit volume proposed is:

$$\psi \left(\Delta, \mathsf{d} \right) = \left(1 - \mathsf{d} \right) \psi^0 \left(\Delta_i \right) - \mathsf{d} \psi^0 \left(\bar{\delta}_{3i} \left\langle -\Delta_3 \right\rangle \right) \tag{19}$$

6

where $\langle \cdot \rangle$ is the MacAuley bracket defined as $\langle x \rangle = \frac{1}{2}(x + |x|)$ and $\bar{\delta}_{ij}$ is the Kronecker delta. The constitutive equation for the interface is obtained by differentiating the free energy with the displacement jumps:

$$\tau_i = \frac{\partial \psi}{\partial \Delta_i} = (1 - \mathsf{d}) D^0_{ij} \Delta_j - \mathsf{d} D^0_{ij} \bar{\delta}_{3j} \langle -\Delta_3 \rangle \tag{20}$$

In the present model, the initial stiffness tensor, D^0_{ij}, is defined as:

$$D^0_{ij} = \bar{\delta}_{ij} K \tag{21}$$

where the scalar parameter K is a penalty stiffness. In the expanded form, the constitutive equation can be written in Voigt notation as:

$$\boldsymbol{\tau} = \left\{ \begin{array}{c} \tau_1 \\ \tau_2 \\ \tau_3 \end{array} \right\} = (1 - \mathsf{d}) K \left\{ \begin{array}{c} \Delta_1 \\ \Delta_2 \\ \Delta_3 \end{array} \right\} - \mathsf{d} K \left\{ \begin{array}{c} 0 \\ 0 \\ \langle -\Delta_3 \rangle \end{array} \right\} \tag{22}$$

The energy dissipation during damage evolution, Ξ, represented in Figure 3 for single-mode loading, can be obtained from:

$$\Xi = -\frac{\partial \psi}{\partial \mathsf{d}} \dot{\mathsf{d}} \geq 0 \tag{23}$$

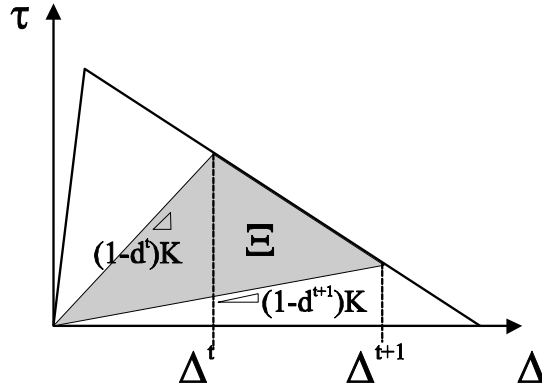The model defined by equation (20) is fully determined if the value of the

Fig. 3. *Energy dissipation during damage evolution*

damage variable d can be evaluated at every time step of the deformation process. For that purpose, it is necessary to define a suitable norm of the displacement jump tensor, a damage criterion, and a damage evolution law, as will be described in the following sections.

2.3.1 Norm of the displacement jump tensor

The norm of the displacement jump tensor is denoted as λ and is also called *equivalent displacement jump norm.* It is used to compare different stages of the displacement jump state so that it is possible to define such concepts as 'loading', 'unloading' and 'reloading'. The equivalent displacement jump is a non-negative and continuous function, defined as:

$$\lambda = \sqrt{\langle \Delta_3 \rangle^2 + (\Delta_{shear})^2} \tag{24}$$

where Δ_3 is the displacement jump in mode I, i.e., normal to midplane, and Δ_{shear} is the euclidean norm of the displacement jump in mode II and in mode III:

$$\Delta_{shear} = \sqrt{(\Delta_1)^2 + (\Delta_2)^2} \tag{25}$$

2.3.2 Damage criterion

The damage criterion is formulated in the displacement jump space. The form of this criterion is:

$$F\left(\lambda^t, r^t\right) := \lambda^t - r^t \leq 0 \qquad \forall t \geq 0 \tag{26}$$

where t indicates the actual time and r^t is the damage threshold for the current time. If r^0 denotes the initial damage threshold, then $r^t \geq r^0$ at every point in time. Damage initiation is produced when the displacement jump norm, λ, exceeds the initial damage threshold, r^0, which is a material property.

A fully equivalent expression for equation (26) that is more convenient for algorithmic treatment is [39]:

$$\bar{F}\left(\lambda^t, r^t\right) := \mathsf{G}\left(\lambda^t\right) - \mathsf{G}\left(r^t\right) \leq 0 \qquad \forall t \geq 0 \tag{27}$$

where $\mathsf{G}(\cdot)$ is a suitable monotonic scalar function ranging from 0 to 1. $\mathsf{G}(\cdot)$ will define the evolution of the damage value, and will be presented in the next section.

2.3.3 Damage evolution law

The evolution laws for the damage threshold and the damage variable must be defined in the damage model. These laws are defined by the rate expressions:

$$\dot{r} = \dot{\mu} \tag{28}$$

$$\dot{\mathsf{d}} = \dot{\mu}\frac{\partial \bar{F}\left(\lambda, r\right)}{\partial \lambda} = \dot{\mu}\frac{\partial \mathsf{G}\left(\lambda\right)}{\partial \lambda} \tag{29}$$

where $\dot{\mu}$ is a damage consistency parameter used to define loading/unloading conditions according to the Kuhn-Tucker relations:

$$\dot{\mu} \geq 0 \quad ; \quad \bar{F}\left(\lambda^t, r^t\right) \leq 0 \quad ; \quad \dot{\mu}\bar{F}\left(\lambda^t, r^t\right) = 0 \tag{30}$$

From the previous equations it is easy to prove [36] that the evolution of the internal variables may be explicitly integrated to render:

$$r^t = \max\left\{r^0, \max_s \lambda^s\right\} \qquad 0 \leq s \leq t \tag{31}$$

$$\mathsf{d}^t = \mathsf{G}\left(r^t\right) \tag{32}$$

which fully describes evolution of the internal variables for any loading/ unloading/ reloading situation. The scalar function $\mathsf{G}(\cdot)$ defines the evolution of the damage value. For a given mixed-mode ratio, β, the function proposed here is defined as,

$$\mathsf{G}(\lambda) = \frac{\Delta^f \left(\lambda - \Delta^0\right)}{\lambda \left(\Delta^f - \Delta^0\right)} \tag{33}$$

Equation (33) defines the damage evolution law by means of a bilinear constitutive equation (see Figure 4), where Δ^0 is the onset displacement jump and it is equal to the initial damage threshold r^0. The initial damage threshold is obtained from the formulation of the initial damage surface or initial damage criterion. Δ^f is the final displacement jump and it is obtained from the formulation of the propagation surface or propagation criterion.
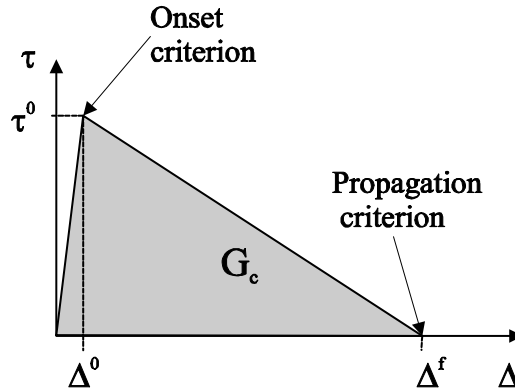

Fig. 4. *A bilinear constitutive equation for the decohesion element for a mixed mode loading situation*

It is therefore necessary to establish the delamination onset and propagation surfaces for the complete definition of the damage model. Delamination onset and propagation surfaces and the damage evolution law fully define the constitutive equations.

The constitutive equations for the interfacial surface are normally developed in a phenomenological way, i.e., satisfying empirical relations that are obtained using experimental results. There are several types of constitutive equations used in decohesion elements: Tvergaard and Hutchinson [40] purpose a trapezoidal law, Cui an Wisnom [41] a perfectly plastic rule, Needleman first presented a polynomial law, [27], and later an exponential law [28]. Goyal et al.[42] adopted Needleman's exponential law to account for load reversal without material healing.

In this paper the law used within the decohesion elements is a bilinear law [21],[24],[43]. The bilinear law is the most commonly used cohesive law due to its simplicity. One drawback of the bilinear law is that the traction-displacement jump relation is discontinuous at its maximum. The discontinuities in the traction-displacement jump relation can be avoided using continuous functions. However, even for such continuous functions, the discontinuity is unavoidable when modeling loading-unloading cycles.

For a given mixed-mode ratio, β, defined as:

$$\beta = \frac{\Delta_{shear}}{\Delta_{shear} + \langle \Delta_3 \rangle} \tag{34}$$

the bilinear constitutive equation is defined by a penalty parameter, K, the damage value, d, the mixed-mode damage initiation, Δ^0 and the total decohesion parameter, Δ^f. These last two values are given by the formulation of the onset and the propagation criterion which takes into account the interaction between different modes and their value depends on the mixed-mode ratio β. The penalty parameter K assures a stiff connection between two neighboring layers before delamination initiation. The penalty parameter should be large enough to provide a reasonable stiffness but small enough to avoid numerical problems, such as spurious tractions oscillations [44], in a finite element analysis. Daudeville et al. [45] have proposed the definition of the penalty stiffness as a function of the interface thickness, t, and elastic moduli of the interface. Zou et al. [4],[46] have proposed a value for the penalty parameter between 10^5 and 10^7 times the value of the interfacial strength per unit length. Camanho and Dávila [24],[47] successfully used a value of $10^6 N/mm^3$, which is smaller than the values proposed by Daudeville et al. [45] and Zou et al. [4],[46].

Propagation criterion

The criterion used to predict delamination propagation under mixed-mode loading conditions is usually established in terms of the energy release rate and fracture toughness. It is assumed that when the energy release rate, G, exceeds a critical value, the critical energy release rate G_c, delamination will grow.

The most widely used criterion to predict delamination propagation under mixed-mode loading, the "power law criterion" is normally established in terms of a linear or quadratic interaction between the energy release rates [48]. However, Camanho et al. [24] shown that using the expression proposed by Benzeggagh and Kenane [35] for the critical energy release rate for a mixed-mode ratio is more accurate for epoxy composites. Using the expression by Benzeggagh and Kenane in [35], the propagation criterion can be written as:

$$G = G_{Ic} + (G_{IIc} - G_{Ic}) \left(\frac{G_{shear}}{G_T}\right)^{\eta} \tag{35}$$

where $G = G_I + G_{shear}$ is the energy release rate under mixed-mode loading and $G_{shear} = G_{II} + G_{III}$ is the energy release rate for shear loading proposed by Li [49],[50].

The propagation surface in the displacement jump space is defined through the final displacements, which are defined from the pure mode fracture toughness (G_{IC}, G_{IIC}, G_{IIIC}) and considering that the area under the traction-displacement jump curves is equal to the corresponding fracture toughness, i.e.:

$$G_C = \frac{1}{2} K \Delta^0 \Delta^f \tag{36}$$

For a given mixed-mode ratio, β, the energy release rates corresponding to total decohesion are obtained from:

$$G_I = \frac{1}{2} K \Delta_3^0 (\beta) \Delta_3^f (\beta) \tag{37}$$

$$G_{shear} = \frac{1}{2} K \Delta_{shear}^0 (\beta) \Delta_{shear}^f (\beta) \tag{38}$$

where $\Delta_{shear}^0 (\beta)$ and $\Delta_3^0 (\beta)$ are respectively the shear and normal displacement jump corresponding to the onset of softening under mixed-mode loading, and $\Delta_{shear}^f (\beta)$ and $\Delta_3^f (\beta)$ are respectively the shear and normal displacement jump corresponding to the total decohesion under mixed-mode loading.

From (34):

$$\Delta_{shear}^0 (\beta) = \Delta_3^0 (\beta) \frac{\beta}{\beta + 1} \tag{39}$$

$$\Delta_{shear}^f (\beta) = \Delta_3^f (\beta) \frac{\beta}{\beta + 1} \tag{40}$$

Using equations (39) and (40) in (37) and (38) the ratio between $\frac{G_{shear}}{G_T}$ can be established in terms of β:

$$\frac{G_{shear}}{G_T} = \frac{\beta^2}{1 + 2\beta^2 - 2\beta} \tag{41}$$

Since the ratio $\frac{G_{shear}}{G_T}$ is only a function of the mixed-mode ratio β, hencefor-ward this ratio is named as B:

$$B = \frac{G_{shear}}{G_T} \tag{42}$$

Using equation (36), (41) and (42) in equation (35) the propagation criterion is obtained in the displacement jump space as:

$$\Delta^f = \frac{\Delta_3^0 \Delta_3^f + \left(\Delta_{shear}^0 \Delta_{shear}^f - \Delta_3^0 \Delta_3^f\right)[B]^\eta}{\Delta^0} \tag{43}$$

Initial damage surface

Under pure mode I, mode II or mode III loading, delamination onset occurs when the corresponding interlaminar traction exceeds its respective maximum interfacial strength, $\tau_3^0, \tau_2^0, \tau_1^0$. Under mixed-mode loading, an interaction between modes must be taken into account. Few models take into account the interaction of the traction components in the prediction of damage onset. The models that account for the interaction of the traction components are usually based on Ye's criterion [51], using a quadratic interaction between modes:

$$\left(\frac{\langle \tau_3 \rangle}{\tau_3^0}\right)^2 + \left(\frac{\tau_2}{\tau_2^0}\right)^2 + \left(\frac{\tau_1}{\tau_1^0}\right)^2 = 1 \tag{44}$$

However, experimental data for the initiation of delamination under mixed-mode is not readily available and consequently, failure criterion that can predict the initiation have not been fully validated.

The criterion for propagation is often formulated independently of the criterion for initiation. In this paper, a link between propagation and initiation is proposed. Since delamination is a fracture process, the initiation criterion proposed in this paper evolves from the propagation criterion and the damage evolution law. The isodamage surface for a damage value equal to 1 corresponds to the propagation surface obtained from equation (35). Then, the isodamage surface for a damage value equal to 0 is the initial damage surface. With these assumptions, the criterion for delamination initiation proposed here is:

$$\left(\tau^0\right)^2 = (\tau_3)^2 + (\tau_1)^2 + (\tau_2)^2 = (\tau_3^o)^2 + \left(\left(\tau_{shear}^o\right)^2 - (\tau_3^o)^2\right)[B]^\eta \tag{45}$$

In the displacement jump space, the criterion becomes:

$$\left(\Delta^0\right)^2 = (\Delta_3)^2 + (\Delta_1)^2 + (\Delta_2)^2 = \left(\Delta_3^0\right)^2 + \left(\left(\Delta_{shear}^0\right)^2 - \left(\Delta_3^0\right)^2\right)[B]^\eta \tag{46}$$

12

The initiation criterion developed here and summarized by equation (45) is compared with Ye's criterion and with a maximum traction criterion, which do not take into account mode interaction. The surfaces obtained by the different criterions are represented in Figure 5. The values predicted by the new criterion are very close to Ye's criterion, that has been successfully used in previous investigations [24].
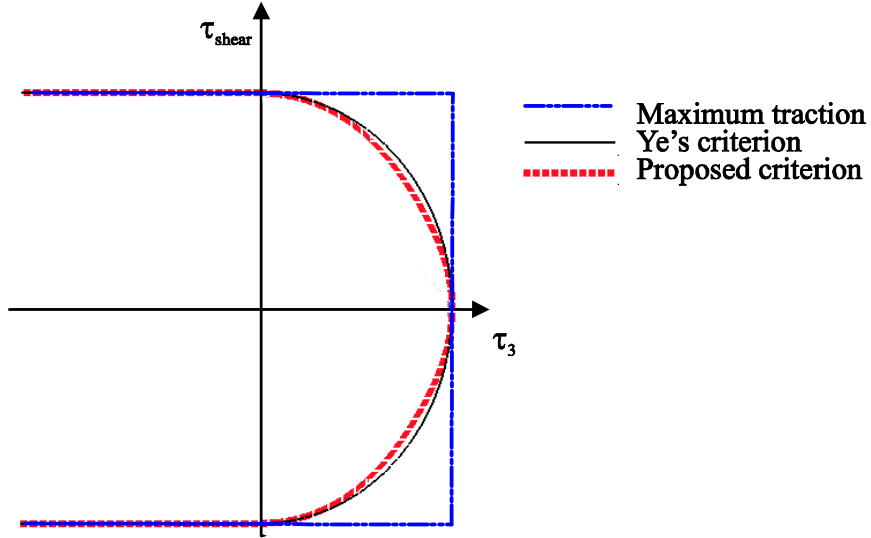

Fig. 5. *Comparision between Ye's criterion, a maximum traction criterion and the new proposed criterion*

The formulation presented assures a smooth transition for all mixed-mode ratios between the initial damage surface to the propagation surface through damage evolution. In Figure 6 it is represented the evolution of the damage surface from the damage initiation surface to the propagation surface for positive values of displacement jumps.

2.4   Formulation of the constitutive tangent tensor

According to equation (16), the constitutive tangent tensor needs to be defined for the formulation of the constitutive laws in the material discontinuity and for the later numerical implementation of the proposed model. The constitutive tangent tensor is obtained from the differentiation of the secant equation (20):

$$\dot{\tau}_i = D_{ij}\dot{\Delta}_j - \bar{\delta}_{ij}K\left[1 + \bar{\delta}_{3j}\frac{\langle-\Delta_j\rangle}{\Delta_j}\right]\Delta_j\dot{\mathsf{d}} \qquad (47)$$
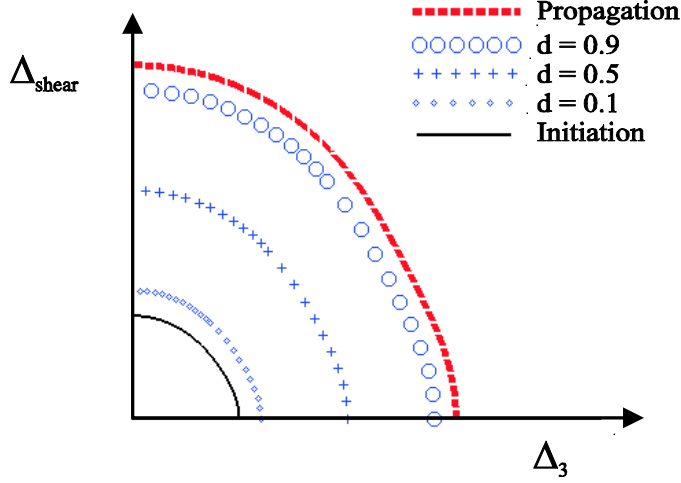
13

Fig. 6. *Damage evolution surface in the relative displacement's space*

where D_{ij} is defined as:

$$D_{ij} = \bar{\bar{\delta}}_{ij} K \left[1 - \mathsf{d} \left(1 + \bar{\bar{\delta}}_{3j} \frac{\langle -\Delta_j \rangle}{\Delta_j} \right) \right] \tag{48}$$

The evolution of the damage variable d only occurs for loading situations. Then, the evolution of the damage variable can be written as:

$$\dot{\mathsf{d}} = \begin{cases} \dot{\mathsf{G}}\left(\lambda\right) = \frac{\partial \mathsf{G}(\lambda)}{\partial \lambda} \dot{\lambda} & , r < \lambda < \Delta^f \\ 0 & , r > \lambda \text{ or } \Delta^f < \lambda \end{cases} \tag{49}$$

where the variation of the function G is obtained assuming that the variation of the final displacement jump Δ^f and the onset displacement jump Δ^0 with the mixed-mode ratio β are not significant for the time increment taken:

$$\frac{\partial \mathsf{G}\left(\lambda\right)}{\partial \lambda} = \frac{\Delta^f \Delta^0}{\Delta^f - \Delta^0} \frac{1}{\lambda^2} \tag{50}$$

The evolution of the displacement norm is obtained from equation (24):

$$\dot{\lambda} = \frac{\partial \lambda}{\partial \Delta_k} \dot{\Delta}_k = \frac{\Delta_k}{\lambda} \left(1 + \bar{\bar{\delta}}_{3k} \frac{\langle -\Delta_k \rangle}{\Delta_k} \right) \dot{\Delta}_k \tag{51}$$

Using equations (49) through (51), equation (47) can be written as:

$$\dot{\tau}_i = D_{ij}^{tan} \dot{\Delta}_j \tag{52}$$

14

$$D_{ij}^{\tan} = \begin{cases} \left\{ D_{ij} - K \left[1 + \bar{\delta}_{3j} \frac{\langle -\Delta_j \rangle}{\Delta_j} \right] \left[1 + \bar{\delta}_{3i} \frac{\langle -\Delta_i \rangle}{\Delta_i} \right] H \Delta_i \Delta_j \right\} & , r < \lambda < \Delta^f \\ D_{ij} & , r > \lambda \text{ or } \Delta^f < \lambda \end{cases} \tag{53}$$

where H is a scalar value given by:

$$H = \frac{\Delta^f \Delta^0}{\Delta^f - \Delta^0} \frac{1}{\lambda^3} \tag{54}$$

3 Finite element discretization - computational model

To transform the strong form of the boundary value problem into a weak form better suited for finite element computations, the displacement u_i must belong to the set $\mathbf{U}$ of the kinematically admissible displacement fields which allows for discontinuous displacements across the boundary Γ_d of the delamination. The weak form of the equilibrium equation is [52]:

$$\int_\Omega \sigma_{ij} \delta \varepsilon_{ij} d\Omega + \int_{\Gamma_d} \tau_i \delta \Delta_m J d\Gamma_d^0 = \int_{\Gamma_F} F_i \delta v_i d\Gamma + \int_\Omega \rho b_i \delta v_i d\Omega \quad \forall v_i \in \mathbf{U} \tag{55}$$

where b_i are the body forces, F_i are surface forces, and equation (14) has been used to relate the initial and the deformed midsurface of the material discontinuity.

The discretization of the domain has been performed by the discretization of the whole domain Ω with standard volume elements. However, the surfaces surrounding the potential delamination Γ_d are discretized with decohesion elements [24]. The discretized formulation is divided in the two domains considering no formal coupling between the continuous and the discontinuous parts of the deformation in the expression for the free energy of the interface [53]. Since the decohesion elements used have zero thickness, the body forces are neglected in these elements. Moreover, it is assumed that no external surface loads are applied. Therefore, the weak form of the internal virtual work for the elements in the surfaces surrounding the potential delaminations can be written as:

$$\int_{\Gamma_d} \tau_i \delta \Delta_m J d\Gamma_d^0 = 0 \tag{56}$$

The displacements and displacement gradients for the decohesion elements are approximated as:

$$u_i|_{\Omega_e} = N_K^e q_{Ki}^e \tag{57}$$

$$[\![u_i]\!] |_{\Omega_e} = \overline{N}_K^e q_{Ki}^e \tag{58}$$

15

where

$$\overline{N}_K^e = \begin{cases} N_K^e & K \in \Gamma_d^+ \\ -N_K^e & K \in \Gamma_d^- \end{cases} \tag{59}$$

where, q_{Ki}^e is the displacement in the i direction of the K node of the element, N_K^e are standard Lagrangian shape functions [52]. $\overline{N}_K^e$ are standard Lagrangian shape functions defined for the decohesion elements [24].

Using equation (58) in equation (56) the weak form of the internal virtual work at current time $t \in R^+$, is given by:

$$\int_{\Gamma_d} \tau_i \hat{B}_{imK} \delta q_{Ki} J d\Gamma_d^0 = 0 \tag{60}$$

where $\hat{B}_{miK}$ is the discrete operator that relates the displacement jump in local coordinates to nodal displacements,

$$\delta \Delta_m = \hat{B}_{imK} \delta q_{Ki} \tag{61}$$

The system of equations given by equation (60) forms the basis for the assumed displacement finite element procedure.

3.1 Discretization of the interfacial surface

3.1.1 Element kinematics

According to equation (57), the displacement field, u_i, and the undeformed material coordinate, X_i, associated to the surfaces $\Gamma_{d\pm}$ are interpolated as follows:

$$u_i^\pm = N_K q_{Ki}^\pm \tag{62}$$

$$X_i^\pm = N_K p_{Ki}^\pm \tag{63}$$

where $q_{Ki}^\pm$ are the nodal displacement vector and $p_{Ki}^\pm$ are the undeformed material nodal coordinate vector. Note that the values of p_{Ki}^- and p_{Ki}^+ can be different in the case that an initial crack exists. Using these equations, the material coordinates of the interfacial midsurface are:

$$\bar{x}_i = \frac{1}{2} N_{Ki} \left(p_{Ki}^+ + p_{Ki}^- + q_{Ki}^+ + q_{Ki}^- \right) \tag{64}$$

The components of the two vectors that define the tangential plane can be written as:

$$v_{\eta_i} = \bar{x}_{i,\eta} = N_{Ki,\eta} \frac{1}{2} \left(p_{Ki}^+ + p_{Ki}^- + q_{Ki}^+ + q_{Ki}^- \right) \tag{65}$$

$$v_{\xi_i} = \bar{x}_{i,\xi} = N_{Ki,\xi} \frac{1}{2} \left(p_{Ki}^+ + p_{Ki}^- + q_{Ki}^+ + q_{Ki}^- \right) \tag{66}$$

16

Using (58) and (12), the displacement jump can then be obtained in local coordinates as:

$$\Delta_m = \Theta_{im} \bar{N}_k q_{Ki} = \bar{B}_{imK} q_{Ki} \tag{67}$$

3.1.2 Element internal force vector and tangent stiffness matrix

The internal force vector of the interface element obtained from equation (60) is given by:

$$f_{Ki} = \int_{\Gamma_{d_i}} \tau_i \hat{B}_{imK} J d\Gamma_c^0 \tag{68}$$

where $\hat{B}_{imK}$ can be written as:

$$\hat{B}_{imK} = \frac{\delta \Delta_m}{\delta q_{Ki}} = \frac{\partial \bar{B}_{jmP}}{\partial q_{Ki}} q_{Pj} + \bar{B}_{imK} \tag{69}$$

The softening nature of the decohesion element constitutive equation causes difficulties in obtaining a converged solution for the non-linear problem. Numerical algorithms such as Newton-Raphson method are used to solve the nonlinear problem. Therefore, the tangent stiffness matrix must be defined. The tangent stiffness matrix stems from the linearization of the internal force vector and it is obtained using Taylor's series expansion about the approximation q_{Ki} [25]. The tangent stiffness matrix, K_{KiZv}, for the decohesion element is:

$$K_{KiZv} = \frac{\partial f_{Ki}}{\partial q_{Zv}} = \int_{\Gamma_d} \frac{d\tau_i}{dq_{Zv}} \hat{B}_{imK} J d\Gamma_d^0 + \int_{\Gamma_d} \frac{d\hat{B}_{imK}}{dq_{Zv}} \tau_i J d\Gamma_d^0 + \int_{\Gamma_d} \frac{dJ}{dq_{Zv}} \tau_i \hat{B}_{imK} d\Gamma_d^0 \tag{70}$$

The computation of the tangent stiffness matrix is intensive and a very accurate expression is not required. Therefore, the second and the third term in the R.H.S of equation (70) are neglected. Thus, the approximate tangent stiffness matrix is:

$$K_{KiZv} \approx \int_{\Gamma_d} \frac{d\tau_i}{dq_{Zv}} \hat{B}_{imK} J d\Gamma_d^0 = \int_{\Gamma_d} \hat{B}_{vjZ} D_{ij}^{\tan} \hat{B}_{imK} J d\Gamma_d^0 \tag{71}$$

where $D_{ij}^{\tan}$ is the material tangent stiffness matrix, or constitutive tangent tensor used to define the tangent stiffness matrix. The constitutive tangent tensor is defined in 2.4.

4 Comparison with experimental studies

The formulation proposed here was implemented in the ABAQUS Finite Element code [54] as a user-written element subroutine (UEL). To verify the

17

element under different loading conditions, the double cantilever beam (DCB) test, the end notched flexure (ENF) test, and mixed-mode bending (MMB) tests are simulated. The numerical predictions are compared with experimental data. The DCB test consists of pure mode I delamination. The ENF tests measure pure mode II interlaminar fracture toughness, and the MMB delaminate under Mixed mode I and II. In the absence of mode III loading, $G_{shear} = G_{II}$. To investigate the accuracy of the formulation in the simulation of delamination DCB, ENF and MMB simulations are conducted for PEEK/APC2, a thermoplastic matrix composite material.

4.1 Mode I, mode II and mixed-mode I and II delamination growth for a PEEK composite

The most widely used specimen for mixed-mode fracture is the mixed-mode bending (MMB) specimen shown in Figure 7, which was proposed by Reeder and Crews [55], [56] and later re-designed to minimize geometric nonlinearities [57]. This test method was recently standardized by the American Society for Testing and Materials [58].
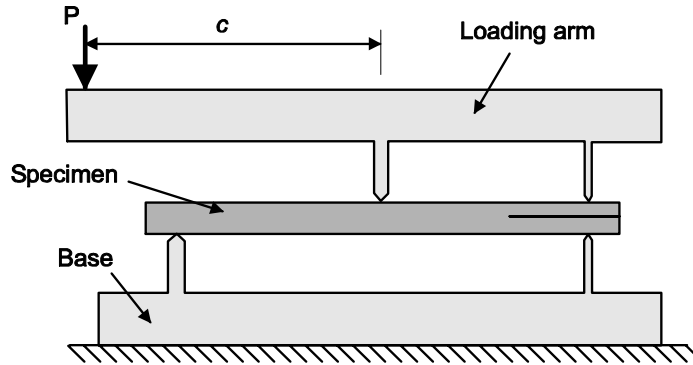

Fig. 7. *MMB test specimen*

The main advantages of the MMB test method are the possibility of using virtually the same specimen configuration as for mode I tests, and the capability of obtaining different mixed-mode ratios, ranging from pure mode I to pure mode II, by changing the length c of the loading lever shown in Figure 7. An 8-node decohesion element is used to simulate DCB, ENF and MMB tests in unidirectional AS4/PEEK carbon-fiber reinforced composite. The specimens simulated are 102-mm-long, 25.4-mm-wide, with two 1.56-mm-thick arms. The material properties are shown in Table 1, and a penalty stiffness $K = 10^6 N/mm^3$ is used.

Table 1. *Properties for PEEK/AS4*

E_{11}	$E_{22} = E_{33}$	$G_{12} = G_{13}$	G_{23}	$\nu_{12} = \nu_{13}$
122.7 GPa	10.1 GPa	5.5 GPa	3.7 GPa	0.25

ν_{23}	G_{IC}	G_{IIC}	τ_3^0	$\tau_2^0 = \tau_1^0$
0.45	0.969 kJ/m^2	1.719 kJ/m^2	80 MPa	100 MPa

The experimental tests were performed at different $\frac{G_{II}}{G_T}$ ratios, ranging from pure mode I loading to pure mode II loading. The initial delamination length of the specimens (a_0) and the mixed-mode fracture toughness obtained experimentally are shown in Table 2.

Table 2. *Experimental data*

G_{II}/G_T	0% (DCB)	20%	50%	80%	100% (ENF)
G_c [kJ/m^2]	0.969	1.103	1.131	1.376	1.719
a_0 [mm]	32.9	33.7	34.1	31.4	39.2

Models using 150 decohesion elements along the length of the specimens, and 4 decohesion elements along the width, are created to simulate the ENF and MMB test cases. The initial size of the delamination is simulated by placing open decohesion elements along the length corresponding to the initial delamination of each specimen (see Table 2). These elements are capable of dealing with the contact conditions occurring for mode II or mixed-mode I and II loading, therefore avoiding interpenetration of the delamination faces. The model of the DCB test specimen uses 102 decohesion elements along the length of the specimen. The different GII/GT ratios are simulated by applying different loads at the middle and at the end of the test specimen. The determination of the middle and end loads for each mode ratio is presented in [24]. The experimental results relate the load to the displacement of the point of application of the load P in the lever (load-point displacement, Figure 7). Since the lever is not simulated, it is necessary to determine the load-point displacement from the displacement at the end and at the middle of the specimen, using the procedure described in [24]. The B-K parameter $\eta = 2.284$ is calculated by applying the least-squares fit procedure proposed in [24] to the experimental data shown in Table 2. Figure 8 shows the numerical predictions and the experimental data for all the test cases simulated, and Table 3 shows the comparison between the predicted and experimentally determined maximum loads. It can be concluded that a good agreement between the numerical predictions and the experimental results is obtained. The largest difference (-8.1%) corresponds to the case of an MMB test specimen with $\frac{G_{II}}{G_T} = 20\%$. This fact is not surprising, since the largest difference between the
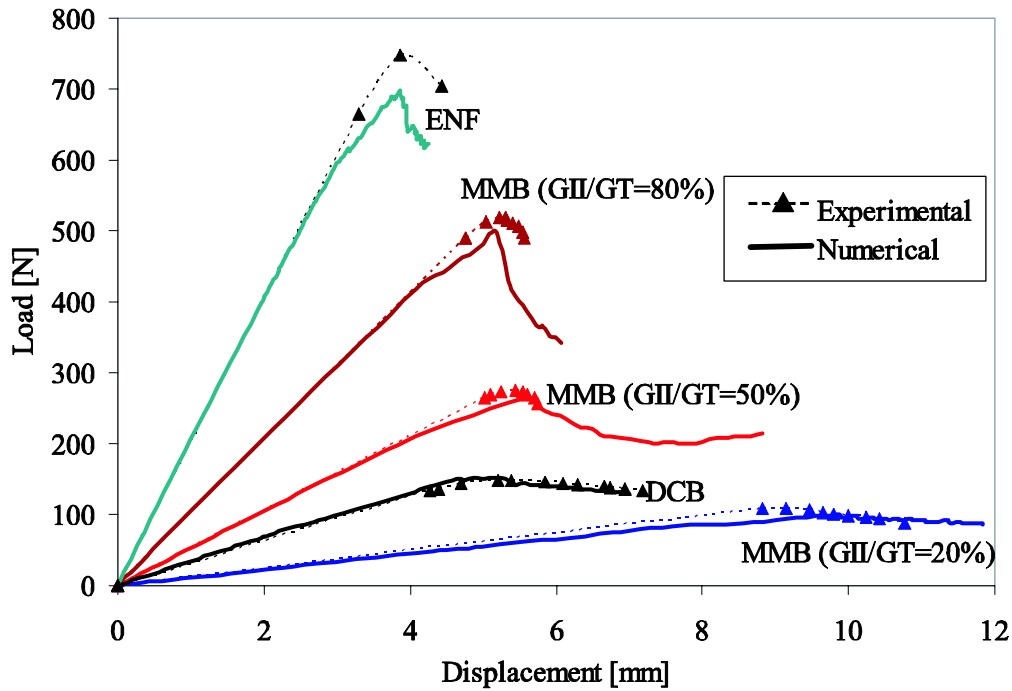
Fig. 8. *Numerical and experimental results*

fracture toughness experimentally measured and the one predicted using the B-K criterion occurs for $\frac{G_{II}}{G_T} = 20\%$ (see [24]).

Table 3 *Comparison of the maximum load*

G_{II}/G_T	Predicted $[N]$	Experimental $[N]$	Error (%)
0% (DCB)	152.4	147.5	3.4
20%	99.3	108.1	-8.1
50%	263.9	275.3	-4.2
80%	496.9	518.7	-4.2
100% (ENF)	697.1	748.4	-6.9

5   Concluding remarks

A thermodynamically consistent damage model for the simulation of progressive delamination based on Damage Mechanics was presented. A constitutive equation for the interface was derived from the variation of the free energy of the interface. The resulting damage model simulates delamination onset and

delamination propagation. The constitutive equation proposed uses a single variable to track the damage at the interface under general loading conditions. A new initiation criterion that evolves from the Benzeggagh-Kenane propagation criterion has been developed to assure that the model accounts for changes in the loading mode in a thermodynamically consistent way and avoids material healing. The damage model was implemented in the finite element code ABAQUS by means of a user-written decohesion element. The material properties required to define the element constitutive equations are the interlaminar fracture toughnesses, the penalty stiffness, and the strengths of the interface. In addition, a material parameter η, which is determined from standard delamination tests, is required for the Benzeggagh-Kenane mode interaction law.

Three examples were presented that test the accuracy of the method. Simulations of the DCB and ENF tests represent cases of single-mode delamination. MMB tests were simulated at various proportions of mode I and II loading conditions. The examples analyzed are in good agreement with the test results and they indicate that the proposed formulation can predict the strength of composite structures that exhibit progressive delamination. Although the examples presented in this work were obtained for composite specimens containing pre-existing delaminations, the formulations can be extended to composite structures without any pre-existing defects.

APPENDIX A

A Algorithm

In this section the algorithm implementation of the previous model is outlined. The algorithm contemplates two different options for the computation of the initiation and propagation surfaces. The first option uses the expression for the critical energy release rate formulated by Benzeggagh and Kenane [35]. The second option uses a Power-law form for the failure criterion, which is widely used in the literature for the simulation of delamination. The Power-law criterion is given by:

$$\left(\frac{G_I}{G_{Ic}}\right)^{\eta} + \left(\frac{G_{II}}{G_{IIc}}\right)^{\eta} = 1 \tag{A.1}$$

Initial data for time t+1

Material properties: $G_{IC}, G_{IIC}, G_{IIIc}, E, \eta, \tau^0_{shear}, \tau^0_3$

Current values: $\Delta_3, \Delta_{shear}, \mathsf{d}^t$

(1) Determine mixed-mode ratios

$$\beta = \frac{\Delta_{shear}}{\langle \Delta_3 \rangle + \Delta_{shear}} \tag{A.2}$$

$$B = \frac{\beta^2}{1 + 2\beta^2 - 2\beta} \tag{A.3}$$

(2) Determine pure mode onset displacements

$$\Delta_i^0 = \frac{\tau_i^0}{K} \qquad i = 3, shear \tag{A.4}$$

(3) Determine mixed-mode onset displacement

$$
\begin{gathered}
\textbf{Benzeggagh} - \textbf{Kenane (BK)} \\
\Delta^0 = \sqrt{(\Delta_3^0)^2 + \left[(\Delta_{shear}^0)^2 - (\Delta_3^0)^2\right][B]^\eta} \\
\textbf{Power law (PL)} \\
\Delta^0 = \frac{\sqrt{1+2\beta^2-2\beta}\,\Delta_3^0\Delta_{shear}^0}{\left[\left((1-\beta)\Delta_{shear}^0\right)^{2\eta} + \left(\beta\Delta_3^0\right)^{2\eta}\right]^{\frac{1}{2\eta}}}
\end{gathered}
\tag{A.5}
$$

(4) Determine mixed-mode final displacements

$$
\begin{gathered}
\textbf{BK} \\
\Delta^f = \frac{2}{K\Delta^0}\left[G_{Ic} + (G_{IIc} - G_{Ic})[B]^\eta\right] \\
\textbf{PL} \\
\Delta^f = \frac{2\left[1+2\beta^2-2\beta\right]}{K\Delta^0}\left[\left(\frac{(1-\beta)^2}{G_{Ic}}\right)^\eta + \left(\frac{\beta^2}{G_{IIc}}\right)^\eta\right]^{-\frac{1}{\eta}}
\end{gathered}
\tag{A.6}
$$

(5) Evaluate displacement jump norm

$$\lambda = \sqrt{\langle \Delta_3 \rangle^2 + (\Delta_{shear})^2} \tag{A.7}$$

(6) Update internal variables

$$r^t = \frac{\Delta^0\Delta^f}{\Delta^f - \mathsf{d}^t\left[\Delta^f - \Delta^0\right]} \tag{A.8}$$

$$r^{t+1} = \max\left\{r^t, \lambda^{t+1}\right\} \tag{A.9}$$

$$\mathsf{d}^{t+1} = \frac{\Delta^f\left(r^{t+1} - \Delta^0\right)}{r^{t+1}\left(\Delta^f - \Delta^0\right)} \tag{A.10}$$

22

(7) Compute tangent stiffness tensor

$$\mathbf{D}^{tan} = \mathbf{D}_s^{tan} + \mathbf{D}_k^{tan} \tag{A.11}$$

where

$$\mathbf{D}_s^{tan} = \begin{bmatrix} (1-\mathsf{d})\,k & 0 & 0 \\ 0 & (1-\mathsf{d})\,k & 0 \\ 0 & 0 & \left(1 - \mathsf{d}\frac{\langle\Delta_3\rangle}{\Delta_3}\right)k \end{bmatrix} \tag{A.12}$$

and $\mathbf{D}_k^{tan}$ depends on the loading/unloading conditions:
IF $\left(\lambda^{t+1} < r^t \text{ or } \Delta^f < \lambda^{t+1}\right)$

$$\mathbf{D}_k^{tan} = 0 \tag{A.13}$$

IF $\left(r^t < \lambda^{t+1} < \Delta^f\right)$

$$\mathbf{D}_k^{tan} = \begin{bmatrix} -kH\Delta_1\Delta_1 & -kH\Delta_1\Delta_2 & -kH\Delta_1\Delta_3\left(\frac{\langle\Delta_3\rangle}{\Delta_3}\right) \\ -kH\Delta_2\Delta_1 & -kH\Delta_2\Delta_2 & -kH\Delta_2\Delta_3\left(\frac{\langle\Delta_3\rangle}{\Delta_3}\right) \\ -kH\Delta_3\left(\frac{\langle\Delta_3\rangle}{\Delta_3}\right)\Delta_1 & -kH\Delta_3\left(\frac{\langle\Delta_3\rangle}{\Delta_3}\right)\Delta_2 & -kH\Delta_3\Delta_3\left(\frac{\langle\Delta_3\rangle}{\Delta_3}\right) \end{bmatrix} \tag{A.14}$$

where for a bilinear constitutive law H is given by equation 54.
(8) Compute tractions

$$\begin{Bmatrix} \tau_1 \\ \tau_2 \\ \tau_3 \end{Bmatrix} = (1-\mathsf{d})\,k \begin{Bmatrix} \Delta_1 \\ \Delta_2 \\ \Delta_3 \end{Bmatrix} - \mathsf{d}k \begin{Bmatrix} 0 \\ 0 \\ \langle-\Delta_3\rangle \end{Bmatrix} \tag{A.15}$$

References

[1] O'Brien, T.K., Murri, G.B., Salpekar, S.A. Interlaminar shear fracture toughness and fatigue thresholds for composite material. *Compos Mater: Fatigue and Fracture, ASTM STP,* **1012**,2, 222-50, 1989.

[2] Moore, D.R. The value of fracture mechanics to industry. *Prospects in Fracture.* Imperial College, 8-9 July. 2003.

[3] Liu, S. Quasi-impact damage initiation and growth of thick-section and toughened composite material. *Int J Solids Struct*, **31**, 3079-3098, 1999.

[4] Zou Z., Reid S.R., Li S., Soden P.D. Modelling interlaminar and intralaminar damage in filament wound pipes under quasi-static indentation. *J. Compos. Mater.*, **36**, 477-499, 2002.

[5] Irwin, G.R. Analysis of stresses and strains near the end of a crack transversing a plate, *J. Appl. Mech.*, **24**, 361-366, 1957.

[6] Rybicki, E.F., Kanninen, M.F. A finite element calculation of stress intensity factors by a modified crack closure integral. *Engineering Fracture Mechanics*, **9**, 931-938, 1977.

[7] Raju, I.S. Calculation of strain-energy release rates with higher order and singular finite elements. *Engineering Fracture Mechanics*, **38**(3),251-274. 1987.

[8] Zou, Z., Reid, S.R., Li, S., Soden, P.D. Mode separation of energy release rate for delamination in composite laminates using sublaminates. *Int. J. Solids Struct.*, **38**, 2597-2613. 2001.

[9] Krueger, R. The virtual crack closure technique: history, approach and applications. *NASA/CR-2002-211628*. 2002.

[10] Rice, J.R. A path independent integral and the approximate analysis of strain concentration by notches and cracks. *J. Appl. Mech*, **35**, 379-386. 1968.

[11] Hellen, T.K. On the method of the virtual crack extension. *Int. J. Num. Meth. Eng.* **9**, 187-207. 1975.

[12] Parks, D.M. A stiffness derivative finite element technique for determination of crack tip stress intensity factors. *Int. J. Fract.* **10**(4),487-502,1974.

[13] Griffith, A.A. The phenomena of rupture and flow in solids. *Philosophical transactions of the Royal Society*, London, Series A. **221**, 163-198. 1921.

[14] Dugdale, D.S. Yielding of steel sheets containing slits. *J. Mech. Phys. Sol.* **8**,100-104. 1960.

[15] Barenblatt, G. The mathematical theory of equilibrium cracks in brittle fracture. *Adv. Appl. Mech.* **7**, 55-129. 1962.

[16] Hillerborg, A., Modéer, M., Petersson, P.E. Analysis of crack formation and crack growth in concrete by means of fracture mechanics and finite elements. *Cement and Concrete Researech.* **6**, 773-782. 1976.

[17] Allix, O., Ladeveze, P., Corigliano, A. Damage analysis of interlaminar fracture specimens. *Comp. Struc.* **31**,66-74. 1995.

[18] Allix, O., Corigliano, A. Modelling and simulation of crack propagation in mixed-modes interlaminar fracture specimens. *Int. J. Fract.* **77**,111-140. 1996.

[19] Schellekens J.C.J., de Borst R. A nonlinear finite-element approach for the analysis of mode-I free edge delamination in composites. *Int. J. Solids Struc.*, **30**(9), 1239-1253, 1993.

[20] Chaboche, J.L., Girard, R., Schaff, A. Numerical analysis of composite systems by using interphase/interface models. *Comp. Mech.* **20**, 3-11. 1997.

[21] Mi, U., Crisfield, M.A., Davies. G.A.O. Progressive delamination using interface elements. *J. Compos. Mater*, **32**, 1246-1272, 1998.

[22] Chen, J., Crisfield, M.A., Kinloch, A.J., Busso, E.P., Matthews, F.L., and Qiu, Y. Predicting Progressive Delamination of Composite Material Specimens Via Interface Elements. *Mechanics of Composite Materials and Structures*, **6,** 301–317. 1999.

[23] Alfano G., Crisfield M.A. Finite element interface models for the delamination analysis of laminated composites: mechanical and computational issues. *Int. J. Numer. Meth. Engng.*, **77**(2), 111-170, 2001.

[24] Camanho P.P., Dávila C.G., de Moura M.F. Numerical Simulation of Mixed-Mode Progressive Delamination in Composite Materials. *Journal of Composite Materials,* **37** (16), 1415-1438, 2003.

[25] Goyal-Singhal, V., Johnson, E.R., Dávila, C.G. Irreversible constitutive law for modeling the delamination process using interfacial surface discontinuities. *Composite Structures*, **64**, 91-105, 2004.

[26] Tvergaard, V., Hutchinson, J.W. The influence of plasticity on mixed-mode interface toughness, *J. Mech. Phys. Solids*, **41**, 119-1135. 1993.

[27] Needleman, A. A continuum model for void nucleation by inclusion debonding. *J. Appl. Mech*, **54**, 525-532, 1987.

[28] Xu X-P, Needleman A. Numerical simulations of fast crack growth in brittle solids. *J. Mech. Phys. Solids*, **42** (9), 1397-1434, 1994.

[29] Yan, A.M., Marechal, E., Ngyen-Dang, H. A finite-element model of mixed-mode delamination in laminated composites with and R-curve effect. *Composites Science and Technology*, **61**, 1413-1427. 2001.

[30] Li, D., Wisnom, M. Modelling damage initiation and propagation composites using interface elements. Presented at the *Computer Aided Design in Composite Material Technology- International Conference.* Southampton, UK. 1994.

[31] Petrossian, Z. and Wisnom, M.R. Prediction of Delamination Initiation and Growth From Discontinuous Plies Using Interface Elements, Composites-Part A, **29**, 503–515. 1998.

[32] Ladevèze, P., Allix, O., Gornet, L., Lévêque, D., et al. A computational damage mechanics approach for laminates: identification and comparisons with experimental results, in *Damage Mechanics in Engineering Materials,* G.Z. Voyiadkjis, J.W.W. Ju, and J.L. Chaboche, Editors. Elsevier Science B.V. 481-499. 1998.

[33] Borg, R., Nilsson, L. Simonsson, K. Modeling of delamination using a discretized cohesive zone and damage formulation. *Composites Science and Technology*, **62**, 1299-1314. 2002.

[34] Jansson, N.E., Larsson, R. A damage model for simulation of mixed-mode delamination growth. *Composite Structures*, **53**, 409-417. 2001.

[35] Benzeggagh, M.L., Kenane, M. Measurement of Mixed-Mode delamination Fracture Toughness of Unidirectional Glass/Epoxy Composites With Mixed-Mode Bending Apparatus. *Composites Science and Technology,* **49**,439-49, 1996.

[36] Simo, J., Ju, J. W. Strain- and stress- based continuum damage model- I. Formulation. *International Journal Solids Structures*, **23**, 821-840, 1987.

[37] Simo, J., Ju, J. W. Strain- and stress- based continuum damage model- II. Computational aspects. *International Journal Solids Structures*, **23**, 841-869, 1987.

[38] Mazars, J. Mechanical Damage and Fracture of Concrete Structures. *Advances in Fracture Research (Fracture 81)*, **4**, 1499-1506. Pergamon Press, Oxford, 1982.

[39] Oliver, J., Cervera, M., Oller, S., Lubliner, J. Isotropic damage models and smeared crack analysis of concrete. *Second International Conference On Computer Aided Analsis And Design Of Concrete Structures,* **2**, 945-958, 1990.

[40] Tvergaard, V., Hutchinson, J.W. The relation between crack growth resistance and fracture process parameters in elastic-plastic solids. *J. Mech. Phys. Solids,* **40***,* 1377-1397, 1992.

[41] Cui, W., Wisnom, M. R. A combined stress-based and fracture-mechanics-based model for predicting delamination in composites. *Composites,* **24,** 467-474, 1993.

[42] Goyal-Singhal, V., Johnson, E.R., Dávila, C.G, and Jaunky, N. An Irreversible Constitutive Law for Modeling the Delamination Process Using Interface Elements. 43rd AIAA/ASME/ASCE/AHS/ASC Structures, Structural Dynamics and Materials Conference, Colorado,USA. 2002.

[43] Reddy Jr., E.D., Mello, F.J. and Guess, T.R. Modeling the Initiation and Growth of Delaminations in Composite Structures. *Journal of Composite Materials*, **31**, 812–831. 1997.

[44] Schellekens J.C.J., de Borst R. On the numerical integration of interface elements. *Int. J. Numer. Meth. Engng.*, **36**: 43-66, 1992.

[45] Daudeville, L., Allix, O., Ladevèze, P. Delamination analysis by damage mechanics. Some applications. *Composites Engineering,* **5**(1), 17-24, 1995.

[46] Zou, Z., Reid, S.R., Li, S. A continuum damage model for delaminations in laminated composites. *J. Mech. Phys. Solids*, **51**, 333-356, 2003.

[47] Camanho, P.P., Dávila, C.G., Pinho, S.T. Fracture analysis of composite co-cured structural joints using decohesion elements. *Fatigue Fract Engng Mater Struct,* **27**,745-757, 2004.

[48] Wu, E.M., Reuter Jr., R.C. Crack extension in fiberglass reinforced plastics. *T. & AM Report No.* 275. University of Illinois, 1965.

[49] Li, J., Sen, J.K. Analysis of frame-to-skin joint pull-off tests and prediction of the delamination failure. *42nd AIAA/ASME/ASCE/AHS/ASC Structures, Structural Dynamics and Materials Conference, Seattle, WA, USA,* 2000.

[50] Li, J. Three-Dimensional effects in the prediction of flange delamination in composite skin-stringer pull-off specimens. *15th Conference of the American Society for Composites Texas, USA:* 2000.

[51] Ye, L. Role of Matrix Resin in Delamination Onset and Growth in Composite Laminates, *Composites Science and Technology,* **33**, 257-277, 1988.

[52] Belytschko, T., Liu, W.K., Moran, B. Nonlinear Finite Elements for Continua and Structures. *John Wiley & Sons, LTD,* 2001.

[53] Larsson, R., Jansson, N. Geometrically non-linear damage interface based on regularized strong discontinuity. *Int. J. Numer. Meth Engng,* **54**, 473-497, 2002.

[54] Hibbitt, Karlsson, Sorense. ABAQUS 6.2 User's Manuals. Pawtucket, U.S.A. 1996.

[55] Crews, J.H., Reeder, J.R. A Mixed-Mode Bending Apparatus for Delamination Testing. *NASA TM* 100662. 1988.

[56] Reeder, J.R., Crews, J.H. Mixed-Mode Bending Method for Delamination Testing. *AIAA Journal* **28**, 1270-1276. 1990.

[57] Reeder, J.R., Crews, J.H. Nonlinear Analysis and Redesign of the Mixed-Mode Bending Delamination Test. *NASA TM* 102777. 1991.

[58] Test Method D6671-01. Standard Test Method for Mixed Mode I-Mode II Interlaminar Fracture Toughness of Unidirectional Fiber Reinforced Polymer Matrix Composites. *American Society for Testing and Materials,* West Conshohocken, PA, USA. 2002.

REPORT DOCUMENTATION PAGE

Form Approved
OMB No. 0704-0188

1. REPORT DATE (DD-MM-YYYY)	2. REPORT TYPE	3. DATES COVERED (From - To)
01- 10 - 2004	Technical Memorandum	

4. TITLE AND SUBTITLE

An Interface Damage Model for the Simulation of Delamination Under Variable-Mode Ratio in Composite Materials

5a. CONTRACT NUMBER

5b. GRANT NUMBER

5c. PROGRAM ELEMENT NUMBER

6. AUTHOR(S)

Turon, Albert; Camanho, Pedro P.; Costa, Josep; and Davila, Carlos G.

5d. PROJECT NUMBER

5e. TASK NUMBER

5f. WORK UNIT NUMBER

23-719-20-40-10

7. PERFORMING ORGANIZATION NAME(S) AND ADDRESS(ES)

NASA Langley Research Center
Hampton, VA 23681-2199

8. PERFORMING ORGANIZATION REPORT NUMBER

L-19060

9. SPONSORING/MONITORING AGENCY NAME(S) AND ADDRESS(ES)

National Aeronautics and Space Administration
Washington, DC 20546-0001

10. SPONSOR/MONITOR'S ACRONYM(S)

NASA

11. SPONSOR/MONITOR'S REPORT NUMBER(S)

NASA/TM-2004-213277

12. DISTRIBUTION/AVAILABILITY STATEMENT

Unclassified - Unlimited
Subject Category 39
Availability: NASA CASI (301) 621-0390 Distribution: Standard

13. SUPPLEMENTARY NOTES

An electronic version can be found at http://techreports.larc.nasa.gov/ltrs/ or http://ntrs.nasa.gov

14. ABSTRACT

A thermodynamically consistent damage model for the simulation of progressive delamination under variable mode ratio is presented. The model is formulated in the context of the Damage Mechanics (DM). The constitutive equations that result from the variation of the free energy with damage are used to model the initiation and propagation of delamination. A new delamination initiation criterion is developed to assure that the formulation can account for changes in the loading mode in a thermodynamically consistent way. Interfacial penetration of two adjacent layers after complete decohesion is prevented by the formulation of the free energy. The model is implemented into the commercial finite element code ABAQUS by means of a user-written decohesion element. Finally, the numerical predictions given by the model are compared with experimental results.

15. SUBJECT TERMS

Progressive delamination; Decohesion elements; Laminated composites; Debonding; Continuum Damage Mechanics

16. SECURITY CLASSIFICATION OF:			17. LIMITATION OF ABSTRACT	18. NUMBER OF PAGES	19a. NAME OF RESPONSIBLE PERSON
a. REPORT	b. ABSTRACT	c. THIS PAGE			STI Help Desk (email: help@sti.nasa.gov)
U	U	U	UU	32	19b. TELEPHONE NUMBER (Include area code) (301) 621-0390

Standard Form 298 (Rev. 8-98)
Prescribed by ANSI Std. Z39.18